HIGH SCHOOL EDITION
Journal of Student Research
Volume 13 Issue 4 (2024)

Parametric Optimization of Magnetohydrodynamic Thrusters for Efficient and Silent Ocean Propulsion

John Joby[1], Vedha Seenivasan[1] and Lohith Somasundaram[1]

[1]Holy Mary High School, India

ABSTRACT

Today's propulsion systems have many problems, majorly noise caused by the propeller, air pollution and injuries caused to marine life. Every day over 60,000 ships sail and each of them travels around 1000kms. These ships affect over 130 species. The average sound level estimated globally from marine traffic is 100 Hz, based on average shipping activity directed from automatic identification system (AIS) data for 2014. Propellers rotate up to 250 revolutions per minute and these propellers are about 25% faster than an average fan, impacting marine life. These propellers can cause more drag, kill various species of fishes and can sometimes mercilessly chop them into pieces. Additionally, they induce cavitation which means they generate bubbles when they revolve and when these bubbles burst, frequencies of up to 20,000 hertz can be generated. Magnetohydrodynamic thruster is a new and evolving type of electric propulsion system which is devoid of moving parts, with aims of creating efficient and silent thrust. In this study, the effect of several electrode parameters such as length, spacing, magnetic field strength, input voltage and surface area on the output thrust are experimentally tested and verified to determine an optimum design. Environmental factors such as salt concentration and water temperature are monitored as well. The optimum parameters in this parametric study can be extrapolated to determine the same for a real life application.

Introduction

Magnetohydrodynamics (MHD) is the study of electrically conducting fluids interacting with an electromagnetic field. It has several applications including usage in pumping of molten metals (19). MHD can help in power generation (7, 18), and when used in a micro-pump can pump blood to maintain blood sugar levels (1). The MHD propulsion system works by accelerating a conductive fluid using the Lorentz force (8). This is the basis of all electromagnetic propulsion systems (6, 15). These thrusters have been proven to be both efficient and silent when compared to traditional propeller-based thruster systems.

The model has a channeled system in which electrodes are placed on opposite sides with permanent magnets placed in which their magnetic field is perpendicular to the electrodes. By providing an electric current across the channel with water of known salinity and a magnetic field orthogonal to the current, an electromagnetic force is produced perpendicular to both electric and magnetic fields. When attached to a vessel, due to this Lorentz force, water is thrusted through the channel and due to Newton's third law the vessel is moved in the opposite direction. The magnetic field in the channel is produced by neodymium magnets.

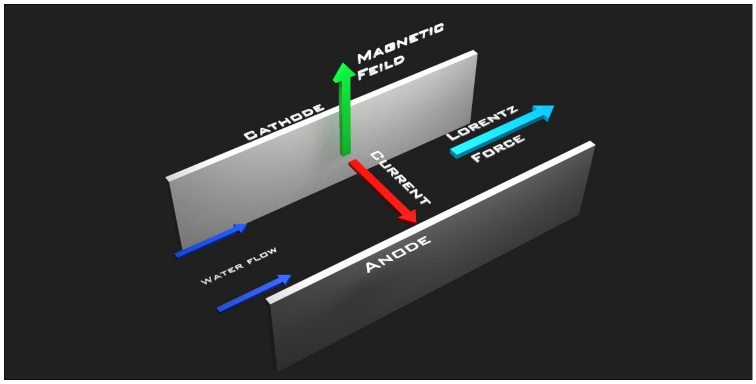

Figure 1. 3D model demonstrating the principle of Lorentz force

The working principle of MHD is completely different from conventional propulsion system using propellers. Due to the lack of any moving parts, this system is not affected by cavitation (14) which is the main reason for drag while using mechanical propellers (3). This system is also silent due to lack of any vibration giving opportunity for usage in stealth missions. This also leads to the vessels achieving higher levels of efficiency. Destruction of marine life is also reduced as the seabed is almost left undisturbed and aquatic creatures are not harmed physically. These qualities are desired by manufacturers in their vessels (5). Reduced fuel costs and zero emissions of greenhouse gasses are other advantages of propulsion using MHD (14, 5). Therefore, this system is a lucrative alternative for the traditional propeller systems (16).

The performance of the MHD marine thrusters is affected by factors such as the current flowing (i), magnetic field strength (b), electrode material (Zn, Brass, Al, Cu), salinity of water passing through the channel, length and surface area of electrodes. The increase in magnetic field strength enhances the electromotive force and increase in salinity reduces the ohmic loss. Adjusting these parameters to an optimum can improve the efficiency. By the method called “seeding” (13), the conductivity of the water can be improved by adding acidic or basic solutions. However, this is out of scope of this article.

By simple physics models and experiments, the effect of velocity due to magnetic field strength, by electrode spacing, salinity, length, current passing through is checked for. It was found that only by using a superconducting electromagnet, any significant thrust can be produced to propel a vessel forward (14, 5).

Literature Review

In the past few decades, Lin et al. (1991,1995) had studied the operation of MHD by using a 1D model and investigated the effects of seawater electrolysis, electrical conductivity enhancements and electrode material on the performance of MHD vessels (12, 2). The helical type MHD was also considered in the study.

Doss et al. had simulated the propulsion system numerically using a 3D MHD flow model and had investigated the effects of magnetic fields in the boundary layer (5, 16). However, the fields were considered in 1D and therefore it was not possible to study the end effects of the MHD. A 1D flow model and a 2D electrical model were coupled to investigate effects of friction and end losses on the performance of the MHD model (4).

At the Chinese Academy for sciences, during the year 2005, a MHD helical channel was simulated using a 3D model for the flow fields and the results were compared with the experiments carried out (11). However, in this experiment the changes of magnetic field around the MHD duct was ignored and rather a fixed field profile was used in the cross-section of the channel.

Shahidian et al. used non-Newtonian fluids (17) for an analytical model of the MHD thruster. Jamalabadi and Park had also solved the equations of the MHD thrusters with AC fields in ranging (9) and non-ranging (10) flows. Although, the end of effects of the 3D model was not considered in their study.

In all the studies carried out few parameters have been left out. This does not give conclusive evidence on the behaviour of the MHD thrusters. There have been semi-2D models and fully 3D models of the thrusters. Therefore, we intend to paint a clear picture using experimental and parametric study.

Analytical Model

It is assumed that all flow fields in the duct — fluid, magnetic, and electric — are unidirectional and constant so that the duct's behavior may be anticipated using an analytical model. In addition to this, the electrical and hydrodynamic properties of the fluid are assumed to remain unchanged. The Lorentz force density in this channel can be determined as:

$$F = J \times B \tag{1}$$

In this equation, F is the Lorentz force density, J is the electric current density, and B is the magnetic flux density. In the analytical model, F, J and B are assumed in x, y, and z directions, respectively. In other words, $F = F \cdot \hat{a}_x$, $J = J \cdot \hat{a}_y$ and $B = B \cdot \hat{a}_z$. Hence, they are considered scalar parameters. The electric current density in the channel can be represented while considering the movement of seawater in the channel and the electrochemical effects, using the Ohm's law:

$$J = \sigma(E_0 - E_t - v_{ex}B) \tag{2}$$

Here, E_0 is the external electric field applied on the electrodes, E_t is the electric field drop caused by the electrochemical effects, v_{ex} is the fluid velocity in the MHD channel and σ is the electrical conductivity of seawater. Substituting equation (2) into (1) gives:

$$F = \sigma(E_0 - E_t - v_{ex}B)B \tag{3}$$

Therefore, the electromagnetic pressure, Δp_e, produced by the MHD channel is determined using:

$$\Delta p_e = FL_1 = \sigma(E_0 - E_t - v_{ex}B)BL_1 \tag{4}$$

Where L_1 is the length of the electrodes. The frictional and local losses cause a portion of the electromagnetic pressure in the MHD channel to drop.

$$\Delta p_{loss} = \left(f_{eq}\frac{L}{D_H} + K\right)\frac{\rho v_{ex}^2}{2} = K_{tot}\frac{\rho v_{ex}^2}{2} \tag{5}$$

Here, Δp_{loss} is the pressure loss, ρ is the seawater density, f_{eq} is the equivalent Darcy friction factor of the electrodes and sidewalls, L is the channel length, DH is the hydraulic diameter of the duct, K is the local loss coefficient, and K_{tot} is the equivalent loss coefficient of the channel. Along the MHD channel, the net pressure can be calculated using:

(6)

$$\Delta p = \Delta p_e - \Delta p_{loss} = \sigma(E_0 - E_t - v_{ex}B)BL_1 - K_{tot}\frac{\rho v_{ex}^2}{2}$$

In this equation, Δp is the net pressure produced by the MHD channel. Then Bernoulli's equation can be used to to write the equation for the pressure drop along the frictionless nozzle axis, Δp_{nozz}.

$$\Delta p_{nozz} = \frac{1}{2}\rho\left(v_{ex}^2 - v_{in}^2\right) \tag{7}$$

Where v_{in} is the fluid velocity at the entrance of the nozzle. The flow rates at the nozzle's inlet and outlet are equal for incompressible fluids.

$$Q = v_{in}A_{in} = v_{ex}A_{ex} \rightarrow \alpha = \frac{v_{ex}}{v_{in}} = \frac{A_{in}}{A_{ex}} \tag{8}$$

Here, A_{in} and A_{ex} are the inlet and outlet areas of the nozzle respectively, α is their ratio and Q is the flow rate. Substituting v_{in} from equation (8) into (7) gives:

$$\Delta p_{nozz} = \frac{1}{2}\rho v_{ex}^2\left(1 - \frac{1}{\alpha^2}\right) \tag{9}$$

The seawater velocity can be determined by considering the net pressure of the MHD channel (Δp) to be equal to the pressure drop along the frictionless nozzle (Δp_{nozz}), and solving this equation:

$$\sigma(E_0 - E_t - v_{ex}B)BL_1 - \frac{\rho}{2}K_{tot}v_{ex}^2 = \frac{\rho}{2}\left(\frac{\alpha^2 - 1}{\alpha^2}\right)v_{ex}^2 \tag{10}$$

The Reynolds number in a marine MHD channel is so large that the friction factor may be considered to be a constant parameter. Hence the fluid velocity can be expressed as:

$$v_{ex} = \sqrt{\frac{2BL_1}{\rho\left(1 - \left(\frac{1}{\alpha^2}\right) + K_{tot}\right)}J} \tag{11}$$

The net force produced in the MHD channel can be shown by:

$$F = \Delta p A_{ex} \tag{12}$$

(Δp) is equal to the pressure drop along the frictionless nozzle (Δp_{nozz}) in the steady state condition. So, substituting from equation (9) and (11) into equation (12) gives:

$$F = BL_1A_{ex}\frac{\left(1 - \left(\frac{1}{\alpha^2}\right)\right)}{\left(1 - \left(\frac{1}{\alpha^2}\right) + K_{tot}\right)}J \tag{13}$$

This equation shows how at a specific electric current density, the net force is not a function of α.

An MHD thruster converts electrical energy into mechanical energy as observed in other electric motors. During this conversion, several types of losses take place, including the overvoltage loss on the surfaces of electrodes, the ohmic loss in the seawater, and the frictional and local losses in the channel. Considering the magnetic field to be created in a lossless way, the input electrical power of the thruster, P_{in}, is:

$$P_{in} = A_{ex} L_1 E_0 J \tag{14}$$

Multiplying the electric potential applied to the electrodes and the total electric current in the channel can also determineP_{in}.

Electrochemical loss of the thruster, P_c, and the ohmic loss, P_O, occurring due to the electrical resistance of the fluid are calculated as follows:

$$P_c = A_{ex} L_1 E_t J \tag{15}$$

$$P_o = A_{ex} L_1 \frac{J^2}{\sigma} \tag{16}$$

Substituting E_0 from equation (2) and J from equation (10) into equations (14) to (16) gives:

$$P_{in} = A_{ex}\left[\frac{\rho^2}{4B^2 L_1 \sigma}\left(1-\left(\frac{1}{\alpha^2}\right)+K_{tot}\right)^2 v_{ex}^4 + \frac{\rho}{2}\left(1-\left(\frac{1}{\alpha^2}\right)+K_{tot}\right) v_{ex}^3 + \frac{\rho E_t}{2B}\left(1-\left(\frac{1}{\alpha^2}\right)+K_{tot}\right) v_{ex}^2\right] \tag{17}$$

$$P_c = \frac{A_{ex}\rho E_t}{2B}\left(1-\left(\frac{1}{\alpha^2}\right)+K_{tot}\right) v_{ex}^2 \tag{18}$$

$$P_o = \frac{A_{ex}\rho^2}{4B^2 \sigma L_1}\left(1-\left(\frac{1}{\alpha^2}\right)+K_{tot}\right)^2 v_{ex}^4 \tag{19}$$

The movement of fluid particles against the rough walls of the channel is called friction loss, Pf, and is calculated as:

$$P_f = f \frac{L_1}{D_H} \frac{\rho}{2} A_{ex} v_{ex}^3 \tag{20}$$

'Local loss', also known as minor loss in the channel, P_m, can be determined by using the following equation. It is caused because of gradual contraction of the nozzle.

$$P_m = K \frac{\rho}{2} A_{ex} v_{ex}^3 \tag{21}$$

The sum of the frictional and minor losses within the MHD channel together are considered to be hydraulic losses (P_h).

The net power that is converted to useful work is known as output power, P_{out}. It depends on the mechanical load of the thruster. It is calculated as shown below:

$$P_{out} = \Delta p Q \tag{22}$$

It has already been stated how Δp is equal to Δp_{nozz} in a steady-state condition. So, substituting from equations (7) and (8) into equation (22) gives:

$$P_{out} = \frac{\rho A_{ex}}{2}\left(1 - \frac{1}{\alpha^2}\right) v_{ex}^3 \tag{23}$$

The overall efficiency of the MHD thruster is defined using the equation:

$$\eta_{tot} = \frac{P_{out}}{P_{in}} = \frac{\Delta p Q}{U_0 I} \tag{24}$$

Here, U_0 is the electric potential applied to the electrodes and I is the total electric current in the channel. Substituting from equations (6) and (8) into (24) gives:

$$\eta_{tot} = \frac{B v_{ex}}{E_0} - \frac{\rho K_{tot} v_{ex}}{2 L_1 E_0 J} \tag{25}$$

Then, substituting E_0 from equation (2) and J from equation (10) into the above equation, the thruster's overall efficiency becomes:

$$\eta_{tot} = \left(1 - \frac{K_{tot}}{1 - \left(\frac{1}{\alpha^2}\right) + K_{tot}}\right) \times \left[1 + \frac{E_t}{B v_{ex}} + \frac{\rho}{2\sigma B^2 L_1}\left(1 - \frac{1}{\alpha^2} + K_{tot}\right) v_{ex}\right]^{-1} \tag{26}$$

By differentiating the equation representing overall efficiency with respect to vex, the efficiency will reach a maximum value at an optimum velocity V_{ex-opt}. This is represented in the following equation:

$$v_{ex-opt} = \sqrt{\frac{2\sigma B L_1 E_t}{\rho\left(1 - \left(\frac{1}{\alpha^2}\right) + K_{tot}\right)}} \tag{27}$$

In closing, the maximum efficiency, η_{max}, at optimum velocity is represented as shown below:

$$\eta_{max} = \left(1 - \frac{K_{tot}}{1 - \left(\frac{1}{\alpha^2}\right) + K_{tot}}\right) \times \left[1 + \sqrt{\frac{2\rho E_t\left(1 - \left(\frac{1}{\alpha^2}\right) + K_{tot}\right)}{\sigma B^3 L_1}}\right]^{-1} \tag{28}$$

3D Model

The above-mentioned straightforward analytical model can be utilized to anticipate how certain loss mechanisms will affect the MHD thrusters' operational efficiency. However, this analytical model is unable to analyze other losses that result from 3D effects in the MHD duct. These three-dimensional impacts include electrical and electrochemical end losses. Because of this, the numerical model discussed in this part assumes a 3D distribution of all fluid, magnetic, and electric flow fields. The following is the set of steady-state MHD marine equations that are applied in this model. Additionally, the fluid is considered to be Newtonian, single-phase, and incompressible.

Mass Continuity

$$\nabla \cdot (\rho U) = 0 \tag{29}$$

Here, U is the velocity vector of the fluid. Seawater flowing in the channel of a marine MHD thruster is an example of an incompressible flow. So, the density changes are negligible leading to the mass continuity equation to be simplified as:

$$\nabla \cdot U = 0 \tag{30}$$

Momentum Conservation

$$\rho\left(u\frac{\partial U}{\partial x} + v\frac{\partial U}{\partial y} + w\frac{\partial U}{\partial z}\right) = -\nabla p + \nabla \cdot \tau + J \times B \tag{31}$$

Where B is the magnetic flux density vector, J is the current density, p is the scalar pressure, and τ is the viscous stress tensor acting on each element. Apart from this, u, v, and w are components of velocity in x, y, and z directions, respectively. To calculate τ in turbulent flows there exists many models, but the enhanced renormalisation group (RNG) $k - \varepsilon$ turbulence model is one of the more commonly used ones. The turbulent velocity μ_t must be determined from the local values of the turbulent kinetic energy k and its dissipation rate ε in order to calculate τ using this model. This can be done as follows:

$$\mu_t = \rho C_\mu \frac{k^2}{\varepsilon} \tag{32}$$

Then, the arrays of stress tensor T_{ij} are calculated as:

$$\tau_{ij} = (\mu_t + \mu)\left(\frac{\partial u_i}{\partial x_j} + \frac{\partial u_j}{\partial x_i}\right) \tag{33}$$

The following transport equations must be solved in order to determine the turbulent kinetic energy k and its dissipation rate ε in equation (32).

$$\rho\left(u\frac{\partial k}{\partial x} + v\frac{\partial k}{\partial y} + w\frac{\partial k}{\partial z}\right) = \frac{\partial}{\partial x}\left(\frac{\mu_t}{\sigma_\varepsilon}\frac{\partial k}{\partial x}\right) + \frac{\partial}{\partial y}\left(\frac{\mu_t}{\sigma_\varepsilon}\frac{\partial k}{\partial y}\right) + \frac{\partial}{\partial z}\left(\frac{\mu_t}{\sigma_\varepsilon}\frac{\partial k}{\partial z}\right) + P_k - \rho\varepsilon \tag{34}$$

$$\rho\left(u\frac{\partial \varepsilon}{\partial x} + v\frac{\partial \varepsilon}{\partial y} + w\frac{\partial \varepsilon}{\partial z}\right) = \frac{\partial}{\partial x}\left(\frac{\mu_t}{\sigma_\varepsilon}\frac{\partial \varepsilon}{\partial x}\right) + \frac{\partial}{\partial y}\left(\frac{\mu_t}{\sigma_\varepsilon}\frac{\partial \varepsilon}{\partial y}\right) + \frac{\partial}{\partial z}\left(\frac{\mu_t}{\sigma_\varepsilon}\frac{\partial \varepsilon}{\partial z}\right) + C_{\varepsilon 1}\frac{e}{k}P_k - C_{\varepsilon 2}\rho\frac{\varepsilon^2}{k} \tag{35}$$

Where the production term P_k in (34) and (35) is:

$$P_k = \mu_t\left\{2\left[\left(\frac{\partial u}{\partial x}\right)^2 + \left(\frac{\partial v}{\partial y}\right)^2 + \left(\frac{\partial w}{\partial z}\right)^2\right] + \left(\frac{\partial u}{\partial y} + \frac{\partial v}{\partial x}\right)^2 + \left(\frac{\partial u}{\partial z} + \frac{\partial w}{\partial x}\right)^2 + \left(\frac{\partial v}{\partial z} + \frac{\partial w}{\partial y}\right)^2\right\} \tag{36}$$

Table 1 contains the values of the constants in this model, which were calculated using empirical data.

Equation of Energy

$$\rho C_v(U \cdot \nabla T) = k\nabla^2 T + \frac{J^2}{\sigma} + \Phi \quad (37)$$

Where k is the working fluid's thermal conductivity, C_v is its specific heat, and T is its temperature. In addition, Φ represents the fluid's viscous dissipation function and $\frac{J^2}{\sigma}$ is the ohmic loss density. For a Newtonian incompressible viscous fluid, such as seawater, Φ is computed as follows:

$$\Phi = \mu\left[2\left(\frac{\partial u}{\partial x}\right)^2 + 2\left(\frac{\partial v}{\partial y}\right)^2 + 2\left(\frac{\partial w}{\partial z}\right)^2 + \left(\frac{\partial u}{\partial y} + \frac{\partial v}{\partial x}\right)^2 + \left(\frac{\partial u}{\partial z} + \frac{\partial w}{\partial x}\right)^2 + \left(\frac{\partial v}{\partial z} + \frac{\partial w}{\partial y}\right)^2\right] \quad (38)$$

Given water's high specific heat, its temperature cannot be appreciably changed by either viscous dissipation or ohmic loss. As a result, the MHD equations' energy equation is disregarded in the marine application.

Turbulent Model Constants	Table 1
Parameter	**Value**
$C\mu$	0.09
$C\varepsilon_1$	1.44
$C\varepsilon_2$	1.92
σk	1.0
$\sigma\varepsilon$	1.3
$C\mu$	0.09

Maxwell's Equations and Ohm's Law

There are just three Maxwell's equations required under MHD approximations.

$$\nabla \times B = \mu_0\mu_r J \rightarrow \nabla \cdot J = 0 \quad (39)$$

$$\nabla \times E = 0 \quad (40)$$

$$\nabla \cdot B = 0 \quad (41)$$

Where the relative permeability of seawater is denoted by μ_r and the permeability of free space by μ_0. The Hall effect does not matter in marine MHD equations, and the expression of Ohm's law is as follows:

$$J = \sigma(E + U \times B) \quad (42)$$

Using equation (40), the electric potential, V, is determined by the following relationship:

$$E = -\nabla V \quad (43)$$

A constant voltage on the electrodes is also used to account for the effects of electrochemical overvoltage.

Parametric Study

Important variables including:

1. The strength of the magnetic field
2. Electrode spacing
3. Electrode length
4. Salinity of the water
5. Voltage, etc.

Were modified during a series of tests. The impacts of the specified parameters on thrust, efficiency, and overall propulsion were understood using the findings from these studies. The parametric study helped obtain optimal configurations for maximizing performance of the MHD drive.

Primarily, cylindrical zinc electrodes were attached to a 14-volt battery and voltage was kept constant at 6 volts. Underneath the water container, two ring-shaped magnets with fairly weak magnetic fields were positioned. The water in the container was made to 100 grams per dm^3. The same procedures were followed for the electrodes made of copper, aluminum, and brass. When the experiments were repeated it was seen that brass was the best material for the electrodes. Electrolysis of the water occurred for the longest duration when brass electrodes were used because the oxide layer of brass also conducts electricity unlike the other materials.

The speed of the water being thrusted was measured by using a partially soluble protein. The movement of the protein was recorded on a camera and imported into a software called "Tracker Online" to find the velocity of the water.

Subsequently, a number of studies were carried out using different electrode lengths keeping voltage constant at 6, salinity at 100g per litre, electrode spacing at 3 cm and 4 neodymium magnets. The length varied from 2 to 12 centimeters, while the breadth and thickness remained constant. This led to the conclusion that the water being propelled was affected by the electrodes' length.

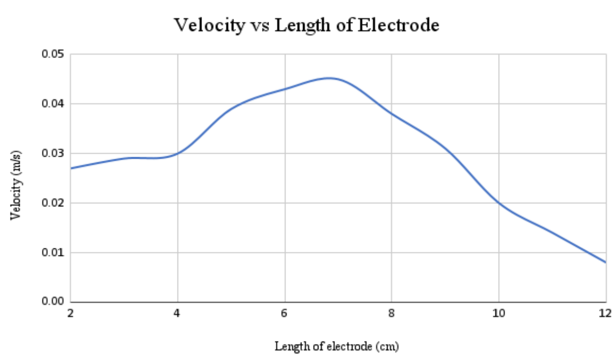

Figure 2. Graph showing the relationship between velocity (V) and length of electrode (cm)

Figure 3. Few of the different electrode lengths which were used

It was also anticipated that the electrode spacing would demonstrate a difference in propulsion. As a result, the distance between the electrodes was varied, and the water's flow velocity was recorded.

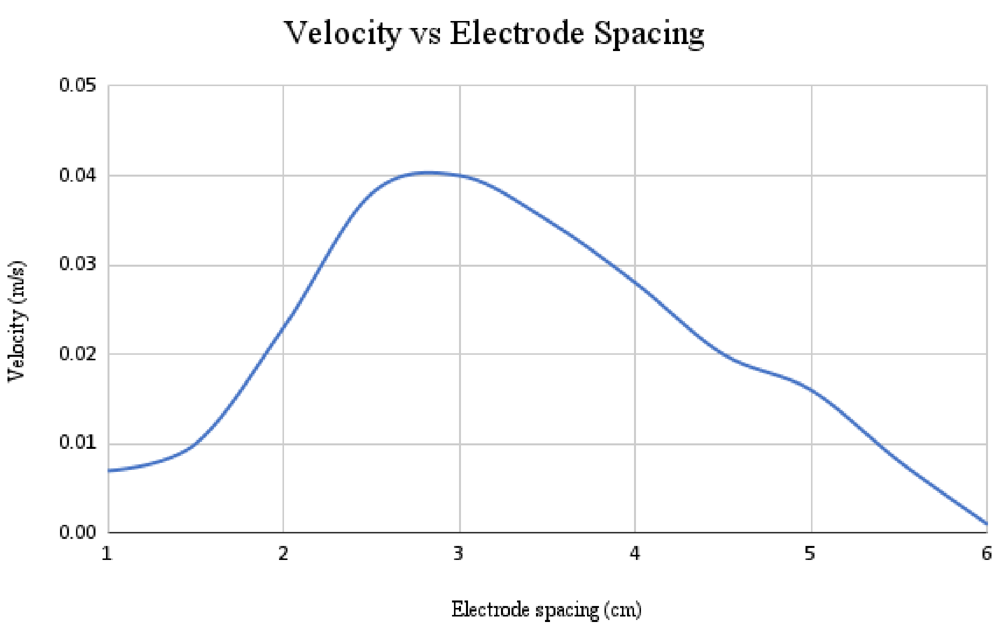

Figure 4. Graph showing the relationship between velocity (V) and space between electrodes (cm)

The graph indicates that when the electrodes were further apart, there was a noticeable increase in velocity till 3 cm but there was a steep drop once the distance was increased above 3 cm.

After confirming that movement of water was possible using MHD, The same tests were conducted again with much stronger magnetic fields. Neodymium magnets were placed above and below the electrodes and the velocity of the water was noticeably more.

Table 2	
No. of Magnets vs Velocity	
No. of Magnets	Velocity (m/s)
2	0.0184
4	0.0404

Since the propulsion of water is because of the formation of ions, the voltage supplied was thought to have an effect on the velocity of water. Experiments were conducted with brass electrodes of length 8 cm, 3 cm apart. These parameters were maintained constant while the voltage was varied from 2 volts to 13 volts. The current was made sure to be the same for more reliable results.

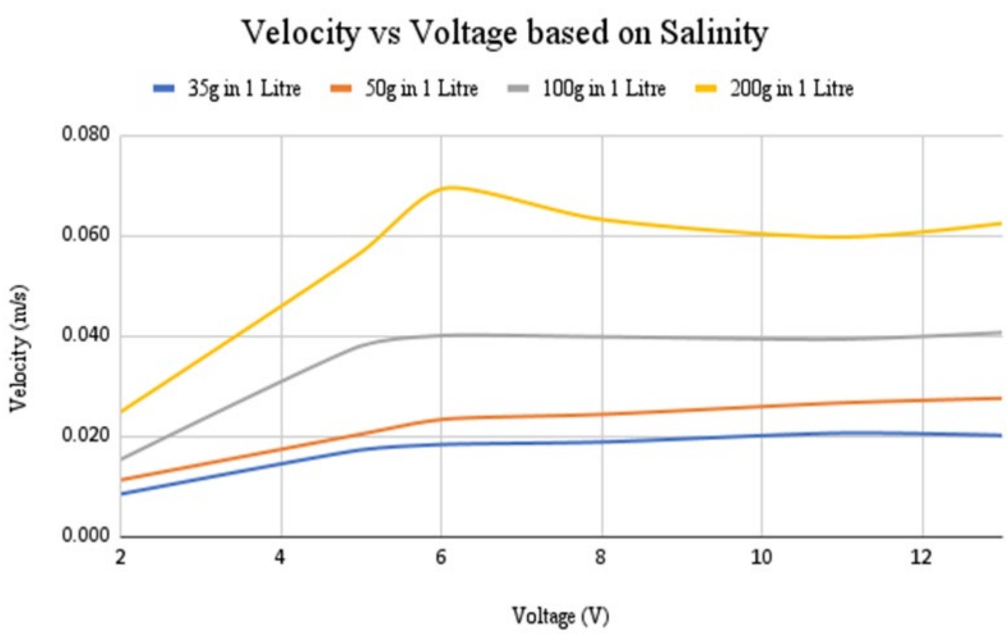

Figure 5. Graph showing the relationship between velocity (m/s) and voltage (V) based on salinity (grams per litre)

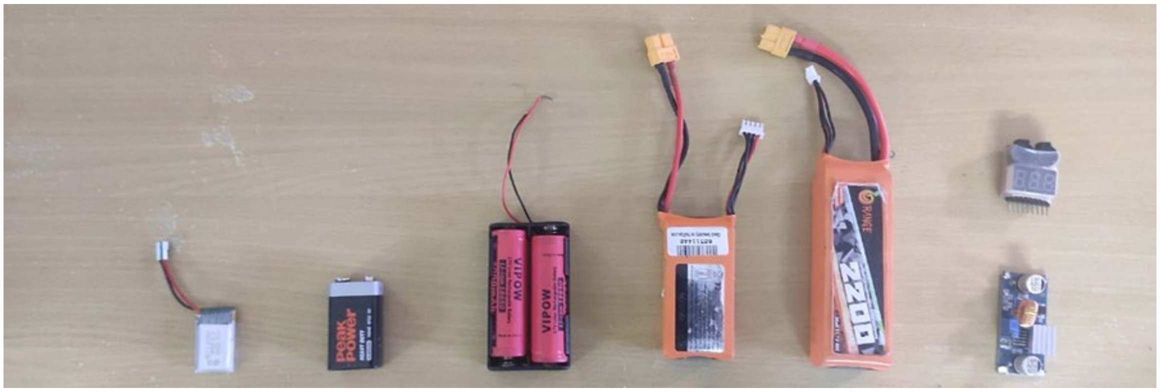

Figure 6. Different power sources used for voltages accompanied with a voltage regulator for accuracy

Using the optimum values obtained from the parametric study, an engine was designed using CAD software. The engine had a convergent nozzle. This was 3D printed. Inside the engine, brass electrodes and neodymium magnets were fitted in.

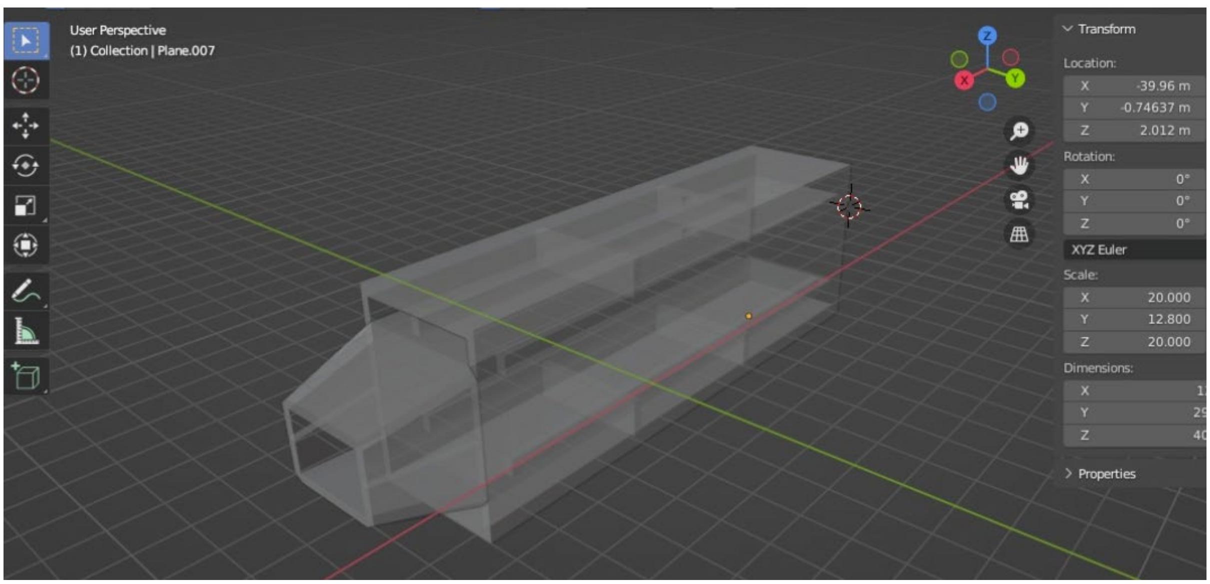

Figure 7. Designing the engine

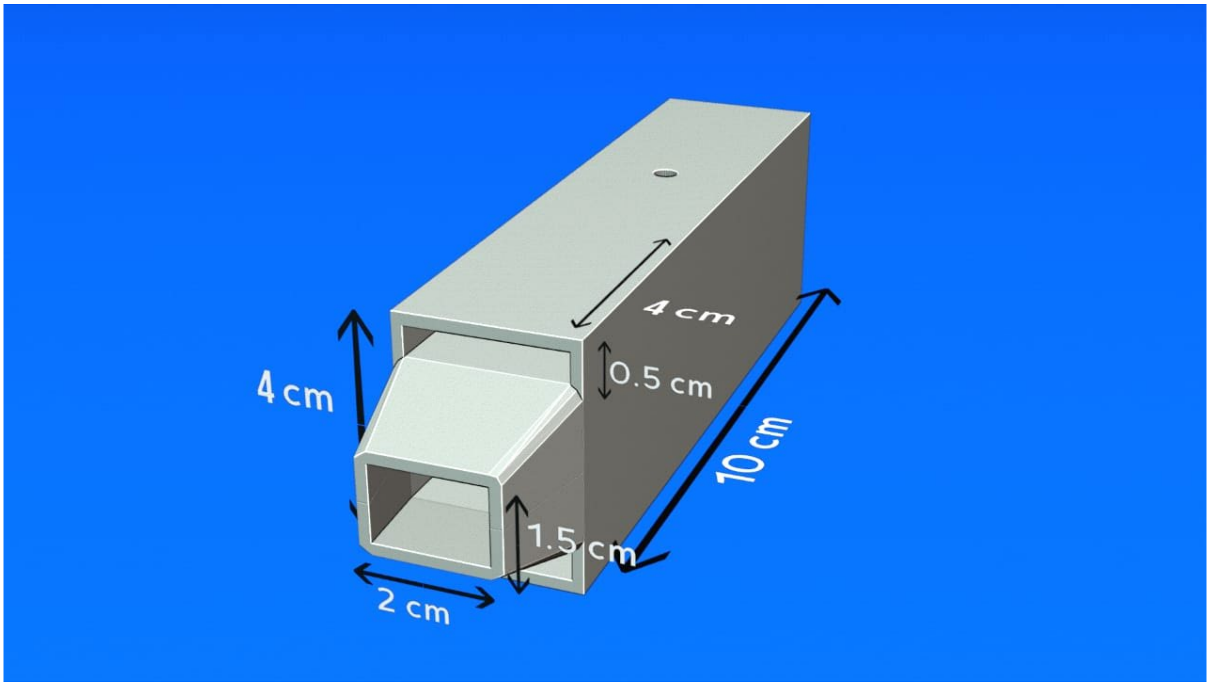

Figure 8. 3D model of the engine design

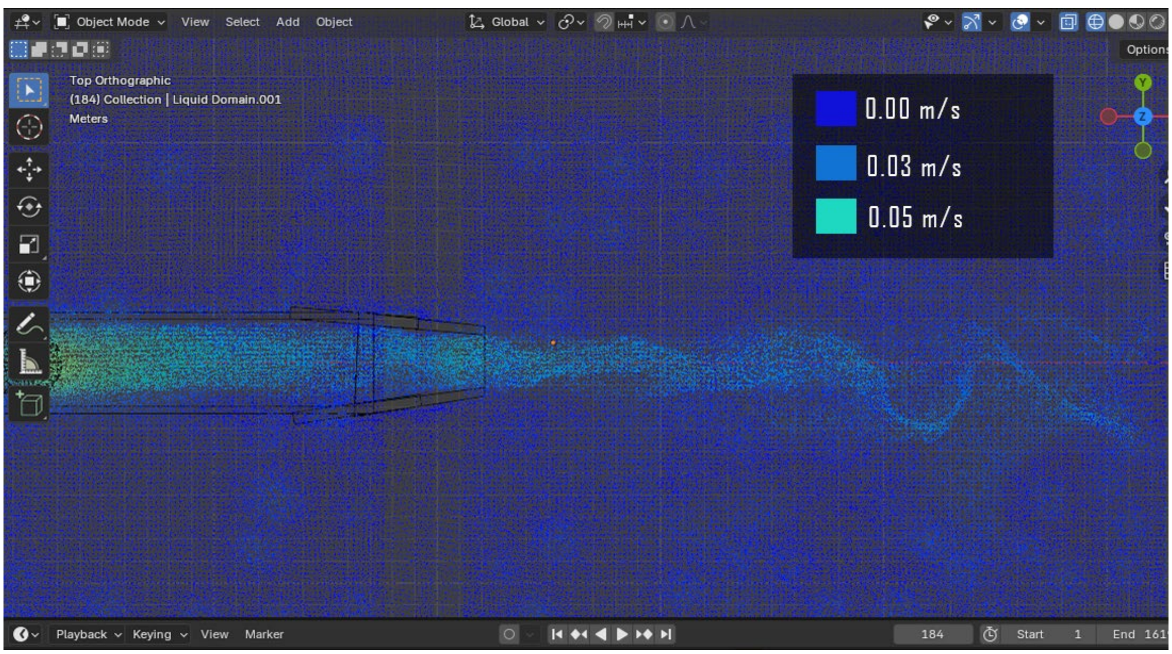

Figure 9. Difference in velocities at different points in the engine

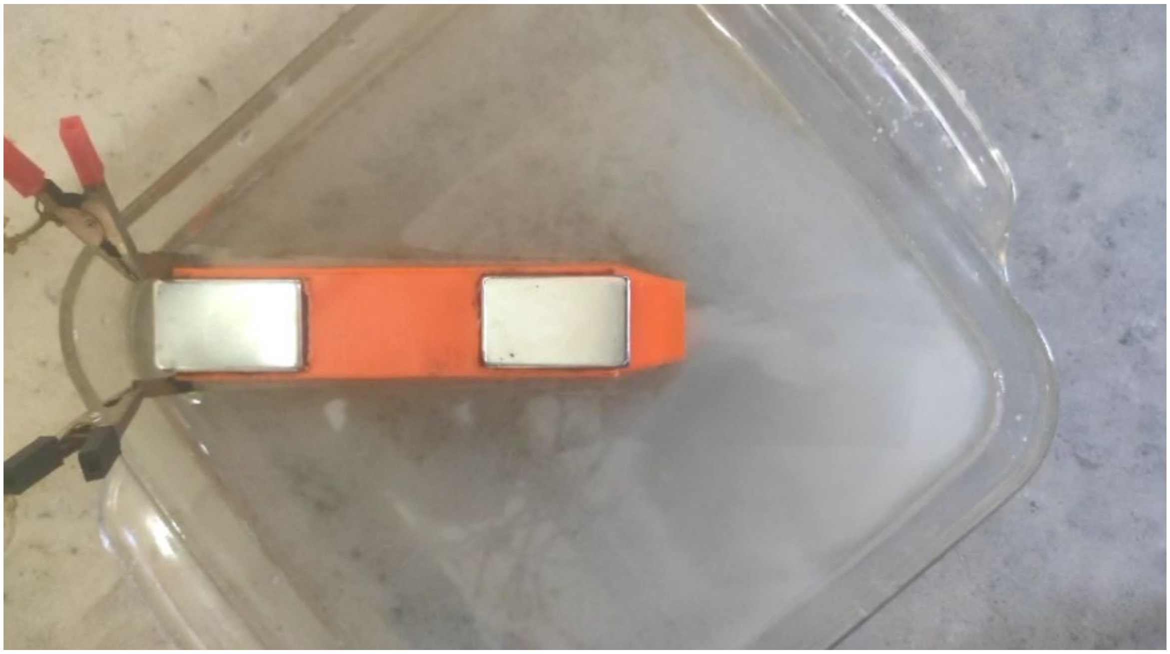

Figure 10. Setup used to test the engine

Now that the engine was ready, the best material and design for boat construction was identified using a series of trials. The parameters taken into consideration were cost effectiveness, weight, hull structure, and performance.

Initially using cardboard boxes, it was clear that neither the material nor the shape was the best as a boat. Following this boats of different sizes and shapes were made from lightweight sponges and then polystyrene.

- Initially a flat streamlined boat was used of different materials
- The size of the streamlined structure was changes to find the best size for the power output we could give
- Then an actual boat with a hull was made using polystyrene
- Finally a catamaran boat was made so that the 3d printed engine can be accommodate with ease apart from the structure giving more stability.

Volume 13 Issue 4 (2024)

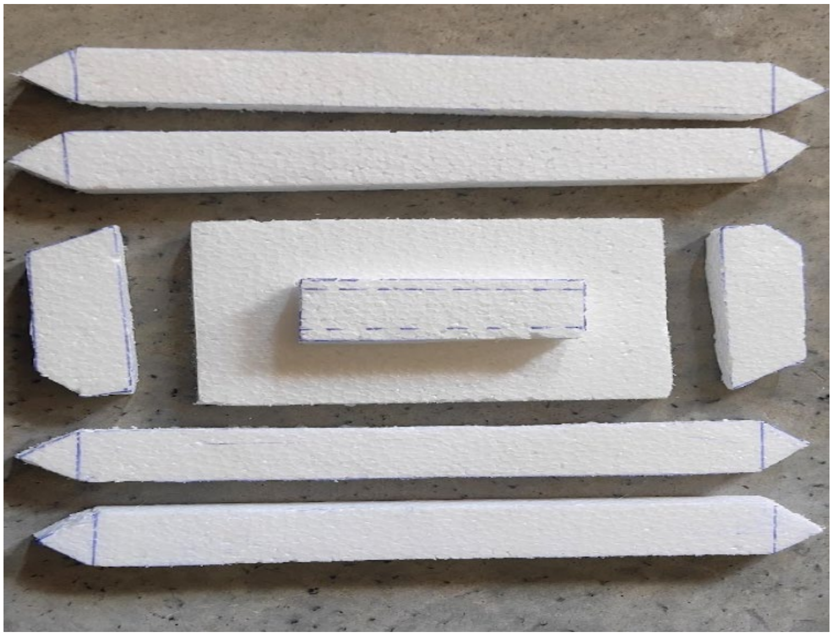

Figure 11. Polystyrene parts of the catamaran boat

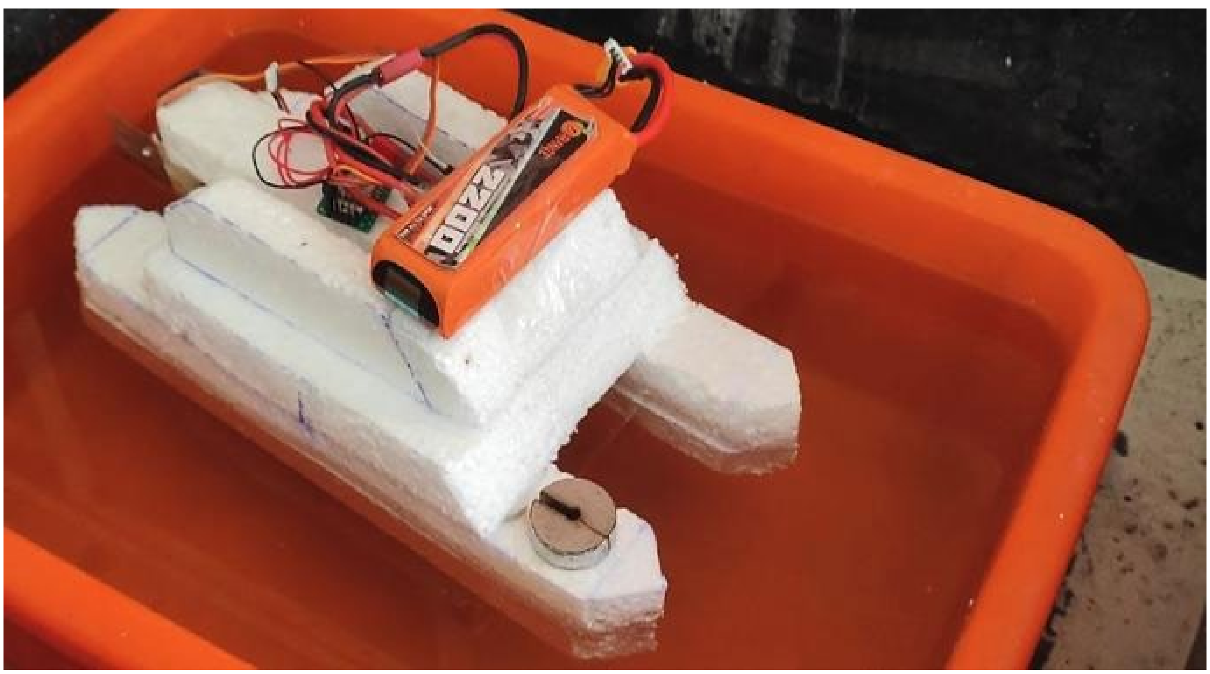

Figure 12. Catamaran boat fitted with the 3D printed engine underneath

Discussion

The potential of magnetohydrodynamic (MHD) thrusters as an environmentally friendly substitute for conventional maritime propulsion systems is highlighted in this paper. The results show that MHD thrusters can function effectively and have a low environmental impact. They also provide a number of advantages over conventional propellers, including the ability to eliminate cavitation and reduce noise pollution. Because of their conductive oxide coating, brass electrodes were discovered to work better; however, large magnetic fields—especially those produced by superconducting magnets—were necessary to provide a substantial amount of thrust.
These encouraging outcomes are not without hurdles, though. The use of superconducting magnets in MHD thrusters raises concerns regarding their scalability and economic viability in large-scale applications due to the additional costs and requirements associated with cryogenic settings. Further research is also necessary to determine the impacts of changing water salinity and the materials' long-term durability.
All things considered, MHD thrusters have enormous potential to transform maritime propulsion by lowering greenhouse gas emissions and increasing efficiency, but further study is required to overcome the financial and technological obstacles preventing their widespread usage. Sustained research in this area has the potential to significantly improve ecologically friendly, economical, and silent maritime transportation.

Conclusion

The novel potential of magnetohydrodynamic (MHD) thrusters as a revolutionary replacement for conventional marine propulsion systems is investigated in this work. The study shows that MHD thrusters can greatly minimize noise pollution and environmental damage because they don't have any moving parts, which solves one of the major problems with conventional propellers. Important conclusions show that in order to maximize thrust and efficiency, electrode material, magnetic field strength, electrode spacing, and water salinity are crucial.

The best electrodes were found to be made of brass since they had higher conductivity and extended electrolysis. Significant propulsion was demonstrated to require strong magnetic fields, especially those produced by superconducting magnets. According to the study, MHD thrusters provide lower fuel expenditures and greenhouse gas emissions, which helps to promote more ecologically friendly and sustainable marine transportation.

All things considered, the results demonstrate that MHD thrusters are a practical, economical, and ecologically friendly form of propulsion. The study makes a strong case for more investigation and advancement of MHD technology, which might completely transform maritime transportation by increasing effectiveness and minimizing environmental impact.

Limitations

There are a few limitations that need to be noted, even if this study shows encouraging results for the application of magnetohydrodynamic (MHD) thrusters in marine propulsion. First off, while the experiment was run on a small scale, it is still unclear if the results can be applied to more extensive commercial applications. Moreover, the utilization of superconducting magnets, which are necessary to attain substantial thrust, poses obstacles concerning expenses, accessibility, and the requirement for cryogenic settings. Additionally, the study concentrated on particular elements like the strength of the magnetic field and the type of electrode. So, it is possible that other factors that could have an impact on performance were ignored, such as the durability of the material over time and the effect of changing water salinity levels. To overcome these obstacles and confirm the viability of MHD thrusters in actual marine settings, more investigation is needed.

Acknowledgments

We would like to sincerely thank everyone who helped us to successfully complete this research project. We would like to express our sincere gratitude to Patitapaban Sahoo, whose knowledge and assistance was extremely helpful during the entire investigation. We also thank Manthan Vidyashram for providing the facilities and resources needed for the experiments.

References

1. Al-Habahbeh O, Al-Saqqa M, Safi M, Khater TA. (2016). “Review of magnetohydrodynamic pump applications”. *Alexandria Engineering Journal.* **55**(2):1347-58. 10.1016/j.aej.2016.03.021.

2. Aumiller Jr D, Gilbert J, Coslo M, Lin T, editors. (1993) “Analytical and experimental studies of the cyclic magnetohydrodynamic thruster designs.” *ISOPE International Ocean and Polar Engineering Conference*; 1993: ISOPE.

3. Carlton J. (2015) “Broadband cavitation excitation in ships.” *Ships and Offshore Structures.* **10**(3):302-7. 10.1080/17445302.2013.793732.

4. Doss E, Geyer H. (1990) “The need for superconducting magnets for MHD seawater propulsion.” *Argonne National Lab.(ANL), Argonne, IL (United States)*; https://doi.org/10.1109/IECEC.1990.748007

5. Doss E, Roy G. (1991) “Flow characteristics inside MHD seawater thrusters.” *Journal of Propulsion and Power.* **7**(4):635-41. 10.2514/3.23331.

6. Faiz J, Sharifian M. (2006) ”Optimal design of an induction motor for an electric vehicle.” *European transactions on electrical power.* **16**(1):15-33. 10.1002/etep.53

7. Hardianto T, Sakamoto N, Harada N. (2008) “Three-Dimensional Flow Analysis in a Faraday-Type MHD Generator.” *IEEE Transactions on Industry Applications.* **44**(4):1116-23. 10.1109/TIA.2008.926234

8. Haghparast M. (2017) “Transient analysis of magnetohydrodynamic seawater thrusters with decaying magnetic field.” *Ships and Offshore Structures*. **12**(5):591-8. 10.1080/17445302.2016.1187971.

9. Jamalabadi MA, Park J. (2014) "Electro-magnetic ship propulsion stability under gusts." *International Journal of Sciences: Basic and Applied Research Sciences.* **14**:421-7.

10. Jamalabadi MYA, Park JH, Lee CY. (2015) "Optimal design of magnetohydrodynamic mixed convection flow in a vertical channel with slip boundary conditions and thermal radiation effects by using an entropy generation minimization method." *entropy.***17**(2):86. 10.3390/e17020086

11. Jiang H, Peng Y, Zhao L, Sha C, Lin Z, Li R, editors.(2008) " Three-dimensional numerical simulation on helical channel MHD thruster." *2008 International Conference on Electrical Machines and Systems;* IEEE.

12. Lin T, Gilbert J. (1995) "Studies of helical magnetohydrodynamic seawater flow in fields up to twelve teslas." *Journal of Propulsion and Power.* **11**(6):1349-55. 10.2514/3.12334

13. Lin T, Marks S, Gilbert J, editors. (1991) "Sea water conductivity enhancement by acid seeding and the associated two-phase flow phenomena." *Int Symp on Superconducting MHD Ship Propulsion (Kobe, Japan);*

14. Mitchell D, Gubser D. (1988) "Magnetohydrodynamic ship propulsion with superconducting magnets." *Journal of Superconductivity.* **1**:349-64 https://doi.org/10.1007/BF00618593

15. Niemelä M, Luukko J, Pyrhönen J, Pyrhönen O, Kaukonen J. (2000) "Position-sensorless direct-torque-controlled synchronous motor drive for ship propulsion." *European transactions on electrical power.* **10**(6):353-60. 10.1002/etep.117

16. Nishigaki K, Sha C, Takeda M, Peng Y, Zhou K, Yang A, et al. (2000) "Elementary study on superconducting electromagnetic ships with helical insulation wall". *Cryogenics.* **40**(6):353-9. 10.1016/S0011-2275(00)00036-1

17. Shahidian A, Ghassemi M, Khorasanizade S, Abdollahzade M, Ahmadi G. (2009) "Flow analysis of non-newtonian blood in a magnetohydrodynamic pump." *IEEE transactions on magnetics.* **45**(6):2667-70. 10.1109/TMAG.2009.2010323

18. Tanaka M, Okuno Y. (2017) "Performance of a Seed-Free Disk Magnetohydrodynamic Generator With Self-Excited Joule Heating in the Nozzle." *IEEE Transactions on Plasma Science.* **45**(3):454-60. 10.1109/TPS.2016.2635961

19. Tawk M, Avenas Y, Kedous-Lebouc A, Petit M. (2013) "Numerical and Experimental Investigations of the Thermal Management of Power Electronics With Liquid Metal Mini-Channel Coolers." *IEEE Transactions on Industry Applications.* **49**(3):1421-9. 10.1109/TIA.2013.2255511